

An evaluation of single pile and pile group behavior under seismic loading in soft ground

Le Bao Quoc^{1*}

¹ Faculty of Engineering and Technology – Dong Thap University

KEYWORDS

Pile foundation
Soft soil
Soil–pile–earthquake interaction
Plaxis 3D simulation
Seismic wave amplification

ABSTRACT

This paper investigates the seismic behavior of single pile as well as pile group in soft soil through three-dimensional finite element simulation. The computational model is developed using Plaxis 3D programme, in which the used geotechnical parameters are obtained from a geotechnical investigation in Dong Thap Province. Seismic loading is modeled as vertically propagating shear waves with a peak ground acceleration (PGA) of 0.07g according to the Vietnamese standard TCVN 9386:2012. The analysis indicates that when single pile is subjected to seismic loading, the maximum shear force and bending moment increase by 42.5% and 62.1%, respectively, compared to static conditions; (2) For a 3×3 pile group with a rigid cap, these corresponding increases are more significant, reaching 192.5% in shear force and 72.4% in bending moment. Although the internal force in group pile is higher, the settlement of group pile reduces approximately 50%, compare to the single pile case, thereby indicating well performance in overall system stability. Moreover, the ground response analysis shows the motion amplification is about 2.0 to 2.5 times within the 6–20 second, emphasizing the effect of wave amplification in soft deposits. The findings highlight that the consideration of soil–pile–seismic interaction in the foundation design is very necessary, advocating the use of nonlinear dynamic modeling to ensure safety and well performance of structures under seismic excitation.

1. Introduction

Vietnam, though not located within the Pacific Ring of Fire-a region of high seismic activity-is still subject to the effects of major earthquakes from surrounding areas. Furthermore, the country lies within a zone characterized by multiple active tectonic faults, including the Lai Chau–Dien Bien, Son La, Red River, Song Ma, and Song Ca faults. In recent years, there has been a notable increase in both the number and frequency of earthquakes recorded in Vietnam, encompassing both natural seismic events and anthropogenically induced earthquakes, such as those associated with hydropower activities. Several earthquakes have had direct impacts on civil structures and transportation infrastructure, thereby heightening the risk of structural failures and substantial economic losses. A recent example includes the discernible effects of a magnitude 7.7 earthquake in Myanmar on Ho Chi Minh City [7].

In the Mekong Delta, subsurface conditions are predominantly composed of soft clay with low bearing capacity. Such soils are highly susceptible to dynamic loading and possess a significant risk of liquefaction during seismic events. Consequently, investigating the mechanical behavior of soft soils under both static and dynamic loads is critical for ensuring structural resilience.

Pile foundations are commonly employed in infrastructure constructed on soft soils and subjected to heavy loads. While most prior studies have primarily focused on the static load-bearing performance of piles, recent seismic occurrences have raised substantial concerns

about the seismic vulnerability of pile foundations in weak soils. The dynamic response of pile foundations is inherently complex, influenced by factors such as nonlinear soil–pile interaction, seismic wave amplification, and group pile effects. These complexities pose significant challenges to geotechnical design and may compromise foundation stability during strong ground motion.

This study presents a numerical investigation into the dynamic response of single piles and pile groups embedded in soft soil under earthquake loading conditions. A three-dimensional finite element analysis was conducted using the Plaxis 3D software. Input parameters were derived from geotechnical data collected in the Dong Thap region of southern Vietnam, which is representative of soft clayey soils with a high potential for seismic-induced liquefaction. The outcomes of the analysis provide critical insights into the performance of pile foundations under seismic loading, offering a scientific basis for the development of appropriate and safe pile foundation design strategies in soft ground conditions.

2. Theoretical background

2.1. Single Pile Analysis

According to Winkler's theory, each soil layer is assumed to interact with its adjacent layers, leading to the modeling of lateral pile behavior using a beam-on-spring system. This approach has proven effective for analyzing pile response under both static and dynamic lateral loading. The springs and dashpots represent the stiffness and

*Corresponding author: lbquoc@dthu.edu.vn

Received 16/05/2025, explanation 21/05/2025, accepted 22/05/2025

Link DOI: <https://doi.org/10.54772/jomc.v15i01.988>

damping characteristics of the soil at specific depths. The soil–pile spring system can be modeled as either linear-elastic or nonlinear, allowing for the simulation of phenomena such as cyclic degradation and rate dependency. However, a major limitation of this model is its inability to account for shear stress transfer between soil layers, and its simplification to a two-dimensional framework, which neglects radial and full three-dimensional interactions.

The p – y curve is commonly employed to characterize the nonlinear stiffness of soil in soil–pile interaction models and is typically established based on experimental data. Matlock [11] proposed p – y curves for soft clay under both static and dynamic loading conditions. The ultimate resistance of the soil per unit length of the pile is determined by taking the smaller value derived from the following two equations.

$$p_u = \left(3 + \frac{\gamma'}{c} x + \frac{I}{d} x \right) cd$$

$$p_u = 9cd \quad (1)$$

γ' denotes the effective unit weight of the soil from the ground surface to the depth of the p – y curve; x is the depth from the ground surface to the p – y curve; c is the undrained shear strength of the soil at depth x ; and d is the characteristic width of the pile—equal to the width for square or rectangular sections, or the diameter for circular piles. Figure 1 illustrates the typical shape of the p – y curve for soft clay as proposed by Matlock [11].

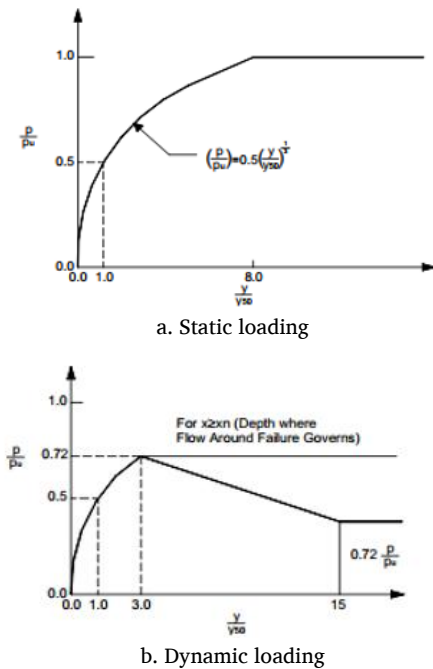


Figure 1. Typical shape of the p – y curve for soft clay [11].

In the case of sandy soils, the ultimate lateral resistance can be determined using Equation (2) as follows:

$$p_u = \gamma H b [K_a (tg^8 \beta - 1) + K_0 \cdot tg \varphi' \cdot tg^4 \alpha] \quad (2)$$

Matlock and Foo, simulated the soil–pile interaction under dynamic loading conditions using a lateral load analysis model for piles based on a dynamic Winkler foundation approach. This model is capable of capturing nonlinear behavior, hysteresis, and degradation effects of the surrounding soil. The pile is modeled as a linearly elastic beam divided into multiple segments, with each segment connected to the soil through a series of springs whose properties vary with depth along the pile. The solution method employs a time-domain finite difference scheme. At each time step, the tangent stiffness between the soil and the pile is updated iteratively, enabling the model to reflect the nonlinear behavior of the soil under seismic excitation. The soil–pile interaction mechanism, illustrated in Figure 2, demonstrates that when the tensile force acting on the pile exceeds the soil's bonding capacity, a gap forms at the contact interface, resulting in a temporary loss of interaction until recontact occurs [10].

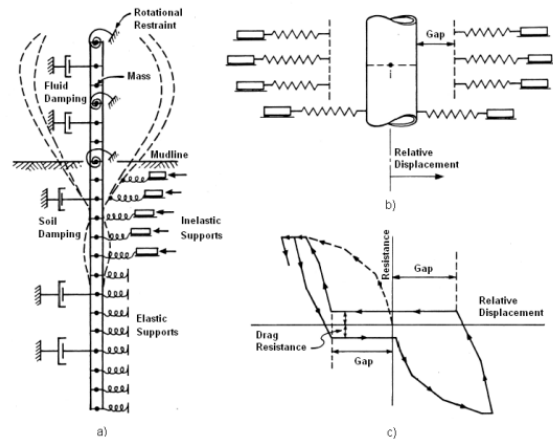


Figure 2. Soil–pile interaction model under seismic loading [10].

2.2. Group Interaction Effects

The load-bearing behavior of pile groups under vertical load (N), lateral load (Q), and moment (M), under both static and dynamic loading conditions, primarily depends on the lateral interaction factors. These factors are influenced by the stiffness ratio between the pile and the soil (E_p/E_s) and the spacing-to-diameter ratio of the piles (S/D). According to El-Sharnouby and Novak [4], the behavior is not significantly affected by pile length or the vertical distribution of soil layers along the pile embedment depth.

Dynamic interaction analysis between pile, soil, and structure in a homogeneous soil medium considers the pile spacing (S), variations in material properties, and a wide range of excitation frequencies. The dynamic interaction factor is defined as the ratio of the additional displacement of a pile caused by a force P to the displacement produced under dynamic loading.

▪ In the case where the pile is subjected to lateral loading, the dynamic interaction factor is determined as follows (according to [4]):

$$\alpha_h^d = \frac{e^{-\frac{\zeta\omega S}{V_{La}}} e^{-\frac{i\omega S}{V_{La}}}}{\sqrt{\frac{2S}{D}}} \quad (2)$$

▪ In the case where the pile is subjected to vertical loading, the dynamic interaction factor is determined as follows (according to [4]):

$$\alpha_v^d = \frac{e^{-\frac{\zeta\omega S}{V_s}}} e^{-\frac{i\omega S}{V_s}} \quad (3)$$

The value of V_{La} is calculated as follows:

$$V_{La} = \frac{3.4v_s}{\pi(1-\nu)} \quad (4)$$

▪ In the general case, the interaction factor depends on the spacing between piles (S) and the angle (β) between the line connecting two piles and the direction of the applied lateral force, as expressed in Equation (6) (according to [4]):

$$\alpha_h^d(\beta) = \alpha_{h0}^d \cos^2 \beta + \alpha_{h90}^d \sin^2 \beta \quad (5)$$

2.3. Wave Propagation Theory, Free-Field Displacement, and Soil Medium

Kelvin-Voigt [8] proposed the constitutive relation between stress and strain as shown in Equation (7). Figure 3 illustrates the Kelvin-Voigt element model [9].

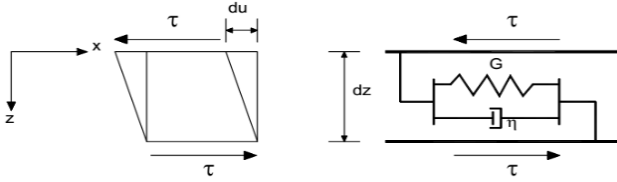


Figure 3. Representation of the Kelvin-Voigt element model [9].

$$\tau = G\gamma + \eta \frac{\partial \gamma}{\partial t} \quad (6)$$

Here, τ denotes the shear stress, γ is the shear strain, and η is the viscous damping coefficient. G represents the shear modulus of the spring under shear stress. In harmonic oscillation, the shear strain can be expressed as:

$$\gamma = \gamma_0 \sin \omega t \quad (7)$$

The damping ratio ξ for the Kelvin-Voigt system is related to the viscous damping coefficient as expressed in Equation (9).

$$\eta = \frac{2G}{\omega} \xi \quad (8)$$

The one-dimensional wave propagation equation in the vertical direction is defined as follows:

$$\rho \frac{\partial^2 u}{\partial t^2} = \frac{\partial \tau}{\partial z} \quad (9)$$

Substituting Equation (7) into Equation (10) with $\gamma = cu/cz$, the displacement equation according to the computational model is obtained as follows:

$$\rho \frac{\partial^2 u}{\partial t^2} = G \frac{\partial^2 u}{\partial z^2} + \eta \frac{\partial^3 u}{\partial z^2 \partial t} \quad (10)$$

Figure 5 illustrates the interaction between the pile and the soil under dynamic loading. Once the free-field displacement is determined, the displacement distribution along the depth and the

length of the pile can be evaluated and is represented by the wave equation form as shown in Equation (12).

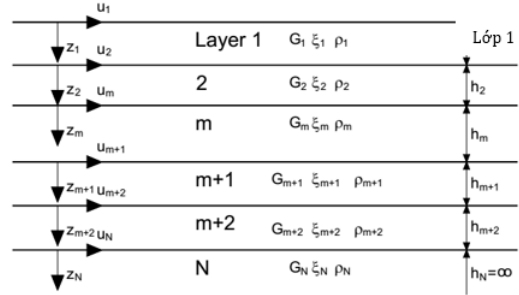


Figure 4. Multi-layer model subjected to horizontal wave propagation [15].

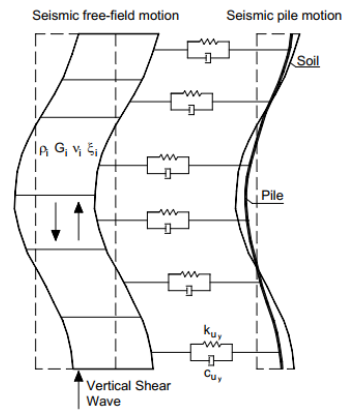


Figure 5. Single pile-soil interaction under dynamic loading [6].

$$u_y(z, t) = (A \cdot e^{ik^*z} + B \cdot e^{-ik^*z}) \cdot e^{i\omega t} \quad (11)$$

Where

A and B are complex functions representing the amplitudes of waves propagating along the z -direction; k^* is the complex stiffness, determined as per Kramer (1996) [8], calculated according to Equations (13):

$$k^* = k_{Re} + ik_{Im} \quad (12)$$

$$k_{Im} = \sqrt{\frac{\rho\omega^2}{2G(1+4\xi^2)}} \left(\sqrt{1+4\xi^2} - 1 \right)$$

$$k_{Re} = \sqrt{\frac{\rho\omega^2}{2G(1+4\xi^2)}} \left(\sqrt{1+4\xi^2} + 1 \right)$$

The displacement equation of the analyzed system is expressed as:

$$[M]\{\ddot{u}\} + [C]\{\dot{u}\} + [K]\{u\} = -[M]\{\ddot{u}_g\} \quad (13)$$

Where, $[M]$, $[C]$, and $[K]$ are the mass, damping, and stiffness matrices of the system, respectively; $\{\ddot{u}_g\}$ is the ground acceleration at the bedrock level.

The mass matrix $[M]$ of the system is given by:

$$M = \begin{bmatrix} m_1 & 0 & 0 & \dots & 0 \\ 0 & m_2 & 0 & \dots & 0 \\ 0 & 0 & m_3 & \dots & 0 \\ \vdots & \vdots & \vdots & \ddots & \vdots \\ 0 & 0 & 0 & \dots & m_n \end{bmatrix} \quad (14)$$

The stiffness matrix $[K]$ of the system is a diagonal and symmetric matrix:

$$K = \begin{bmatrix} k_1 & -k_1 & 0 & \cdot & 0 \\ -k_1 & k_1 + k_2 & -k_2 & \cdot & 0 \\ 0 & -k_2 & k_2 + k_3 & \cdot & 0 \\ \cdot & \cdot & \cdot & \cdot & -k_n \\ 0 & 0 & 0 & -k_n & k_n \end{bmatrix} \quad (15)$$

The damping matrix $[C]$ is defined using Rayleigh damping coefficients.

$$[C] = \alpha_R [M] + \beta_R [K] \quad (16)$$

where α_R, β_R are the Rayleigh damping coefficients, respectively. The mode shapes and natural frequencies are obtained by solving the following equation:

The relative displacement of the soil in the i -th mode of vibration is determined by the following expression:

$$[K]\{\phi\} = \omega^2 [M]\{\phi\} \quad (17)$$

The relative displacement of the soil in the i -th mode of vibration is determined by the following expression:

$$u_i = \frac{1}{\omega_i^2} \Gamma_i S_e \phi_i \quad (18)$$

3. Model and numerical analysis

3.1. Description of the Simulation Problem

This study investigates the dynamic behavior of single piles and pile groups. The single pile is analyzed under two boundary conditions: free head and fixed head. The pile group consists of a square configuration with a rigid cap, comprising 9 piles. All piles are assumed to be linearly elastic, with a diameter $d = 350$ mm and a length $L = 22$ m, embedded in different soil layers as shown in Figures 10 and 16. The soil – pile – foundation system is subjected to seismic loading modeled as vertically propagating shear waves with a peak ground acceleration $a_g = 0.07$ g, using the artificial acceleration time history illustrated in Figure 9.



Figure 6. Perspective view of the Dong Thap provincial Public Administration Center project.

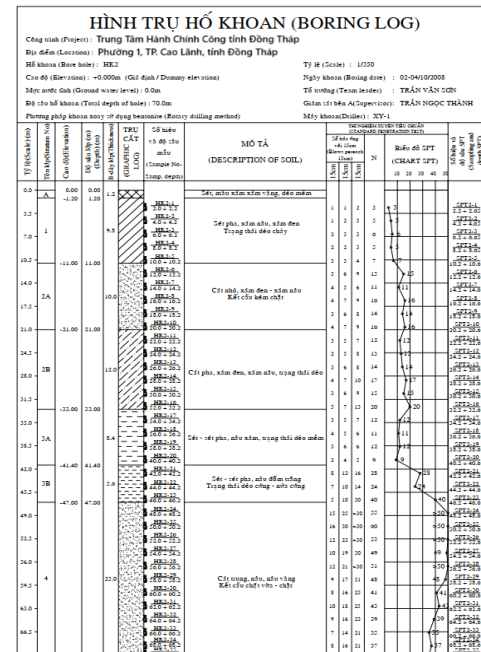


Figure 7. Geological column cross-section of the study area.

Table 1. Soil parameters and pile material properties.

Materials	Depth (m)	Model	Unit Weight γ (kN/m ³)	Elastic Modulus E' (kPa)	Poisson's Ratio ν	Cohesion c (kPa)	Friction Angle ϕ (độ)	Behavior
Layer A. Soft plastic yellow-gray clay	0 – 1,2							
Layer 1: Clayey silt, brown-gray, gray-black, in a plastic-flow state	1,2 - 11	MC	17,5	1200	0,3	10,3	4,95	Undrained
Layer 2A: Fine sand, dark gray to brown-gray, poorly compacted;	11 - 21	MC	18,4	2210	0,3	4,1	25,53	Drained
Layer 2B: Sandy silt, dark gray to brown-gray, plastic state;	21 - 33	MC	18,2	1310	0,3	11,4	17,9	Drained
Layer 3A: Clay-clayey silt, brown-gray, soft plastic state;	33 – 41,4	MC	17,6	1420	0,3	14,9	8,22	Undrained
Layer 3B: Clay-clayey silt, brown with white spots, stiff to semi-stiff plastic state;	41,4 - 47	MC	20,3	1200	0,3	40	15	Undrained
Layer 4: Medium sand, brown to yellow-brown, medium to dense compactness;	47 - 70	MC	20,1	1200	0,3	3,3	30,4	Drained
5. Reinforced Concrete Piles (RC piles).		LEM	25	3×10^7	0,15			Nonporous

The author utilized the commercial software Plaxis 3D version 2024.2.0.1144 to perform the simulations, incorporating an artificially generated acceleration time history corresponding to a peak ground acceleration $a_g = 0.07\text{ g}$. The time scaling is based on the elastic response spectrum according to the Vietnamese standard TCVN 9386:2012. The artificially generated acceleration time history is shown in Figure 8 [13]. The numerical problem was solved using absorbing boundary conditions with a boundary distance of 150 - 200D, following the recommendations of the German Geotechnical Society. Additionally, the interaction between the pile and sliding soil was considered based on the *Rinter* condition in Plaxis.



Figure 8. Time scaling chart based on the elastic response spectrum in TCVN 9386:2012.

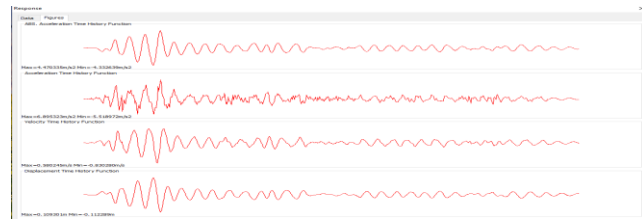


Figure 9. Artificially generated time histories of ground acceleration, velocity, and displacement in Dong Thap corresponding to a peak ground acceleration $a_g = 0.07\text{ g}$.

3.2. Results

a. Single Pile Analysis Results

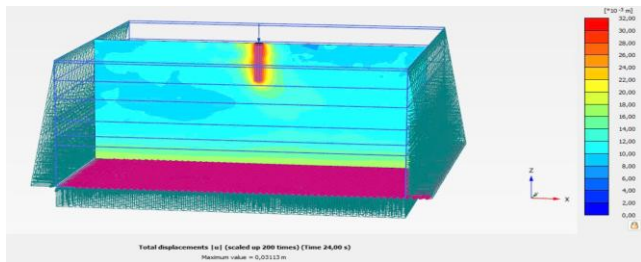


Figure 10. Numerical model of the problem.

From the problem model in Figure 10, the secondary data in Table 1, and the artificial acceleration time history in Figure 9, the internal force values under static and seismic loading show substantial differences—an increase of 42.48 % in shear force and 62.13 % in bending moment, as summarized in Table 2. The differences in

internal force distribution along the pile length between static and seismic loading are illustrated in Figures 12 and 13. The time-history of horizontal displacement uxu_xux indicates that the displacement at the pile head is greater than at the tip, which aligns with the seismic wave amplification behavior in elastic soil model (Figure 14), while the vertical displacement uzu_zuz remains relatively uniform due to the pile's stiffness characteristics (Figure 15).

Table 2. Internal force values of the single pile.

Load Type	Q_{\max} (kN)	M_{\max} (kN.m)
Static Load	3.25	4.28
Dynamic Load	5.64	11.31
Deviation %	42.48 (%)	62.13 (%)

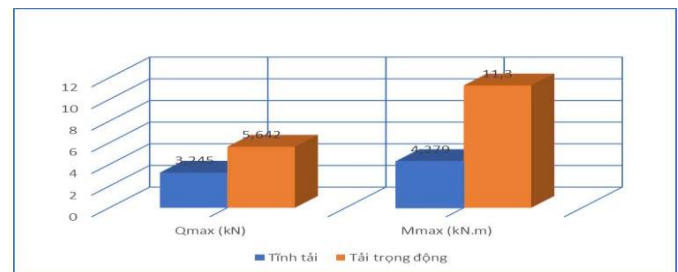


Figure 11. Variation in internal force values of the single pile.

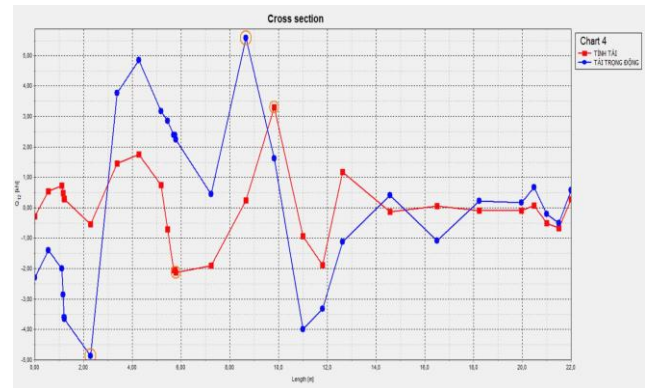


Figure 12. Shear force distribution along the embedded depth of the pile.

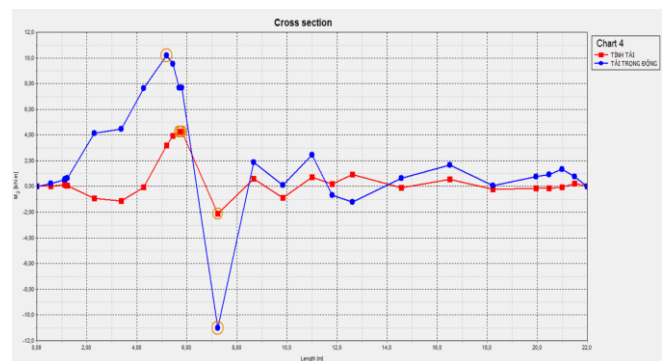


Figure 13. Bending moment (M) distribution along the embedded depth of the pile.

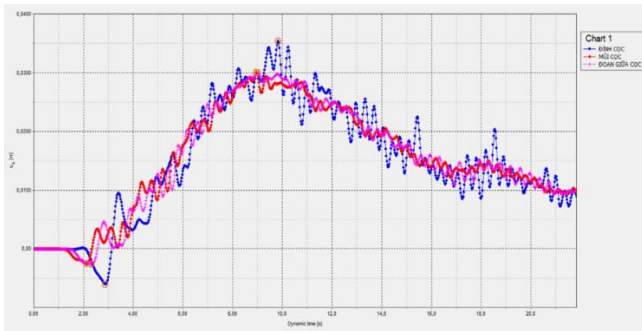


Figure 14. Horizontal displacement u_x at the head, mid-length, and tip of the single pile in soft soil.

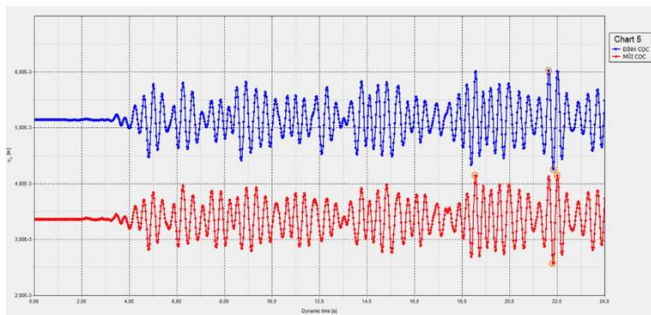


Figure 15. Vertical displacement u_z at the head, mid-length, and tip of the single pile in soft soil.

The analysis results of the pile – soil system under seismic excitation with a peak ground acceleration of $a_g = 0.07$ g; show that, in the case of a single pile, there is a noticeable difference in displacement between the pile head and the tip. The maximum horizontal displacement at the pile head, $|u| = 6$ cm, occurs at $t = 21.6$ seconds. Whereas the maximum displacement at the pile tip, $|u| = 4.3$ cm, appears earlier at $t = 18.3$ seconds and recurs at $t = 22$ seconds. The horizontal displacement of the pile follows a push-pull pattern corresponding to the time-varying ground acceleration.

b. Analysis Results of the 9-Pile Group

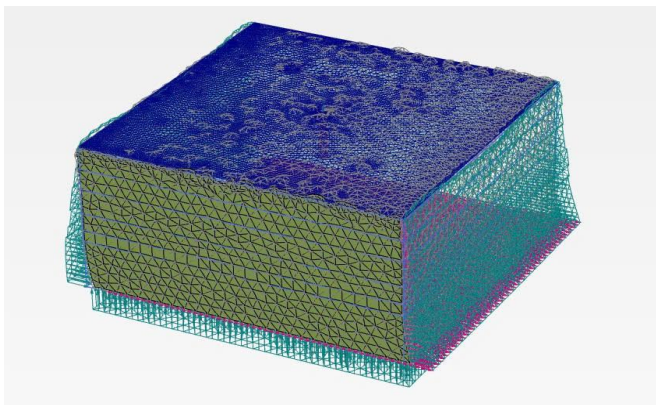


Figure 16. 3D model of the 9-pile group problem.

Similarly, the calculations for the case of a group of 9 piles show the differences in the distribution of shear force and bending moment along the pile length, as illustrated in Figures 18–19. The amplification of ground acceleration in the elastic soil at the ground surface compared to the bedrock is shown in Figure 21.

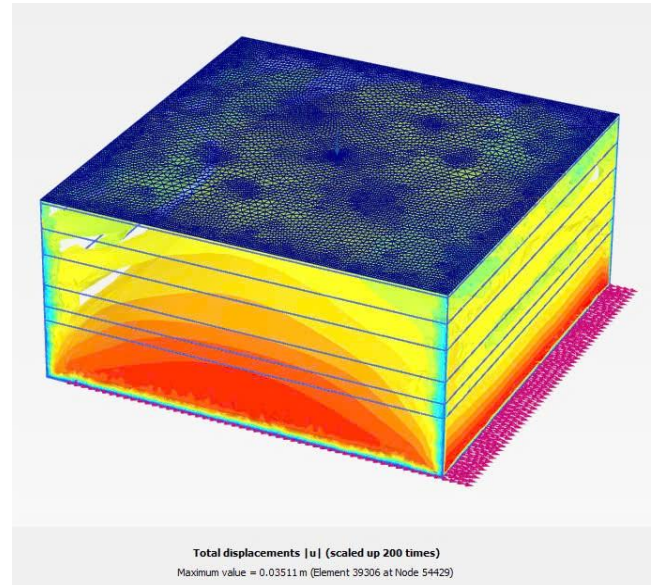


Figure 17. Total displacement of the 9-pile group.

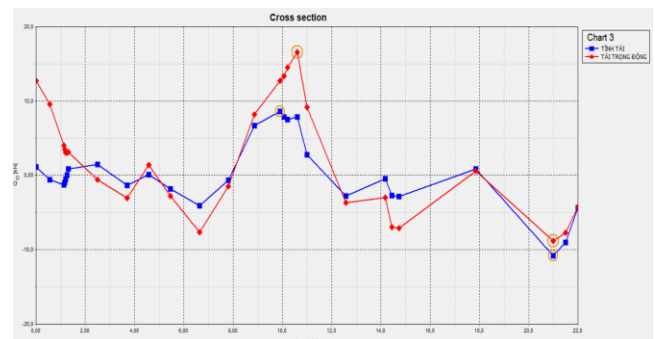


Figure 18. Shear force distribution along the embedded depth of the pile group.

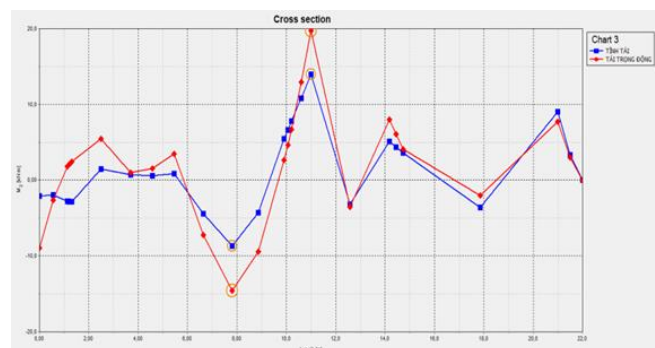


Figure 19. Bending moment distribution along the embedded depth of the pile group.

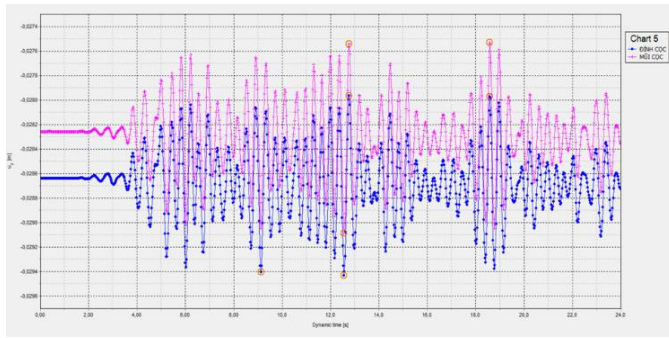


Figure 20. Vertical displacement u_z at the pile head and tip according to the ground acceleration.

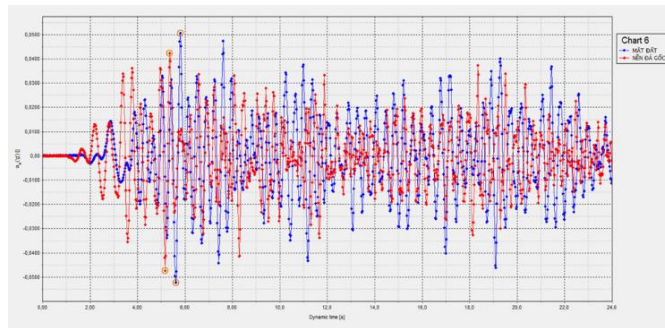


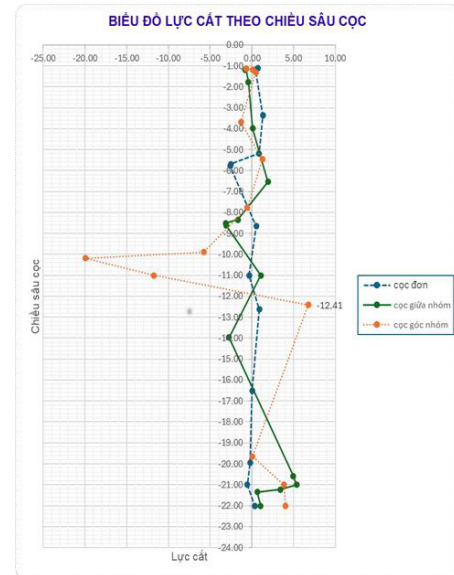
Figure 21. Vertical displacement u_z at the pile head and tip according to the ground acceleration.

For the 9-pile group–soil system under seismic loading with a peak ground acceleration of $a_g = 0.07$ g, the analysis shows that the displacement at the pile head and tip are similar. The maximum displacement at the pile head occurs at $t = 9.1$ seconds and recurs multiple times at $t = 12.5$, $t = 12.7$, and $t = 18.4$ seconds. Similarly, the maximum displacement at the pile tip occurs at $t = 12.8$ seconds and recurs at $t = 18.6$ seconds. The horizontal displacement of the piles follows a push–pull pattern corresponding to the time history of ground acceleration.

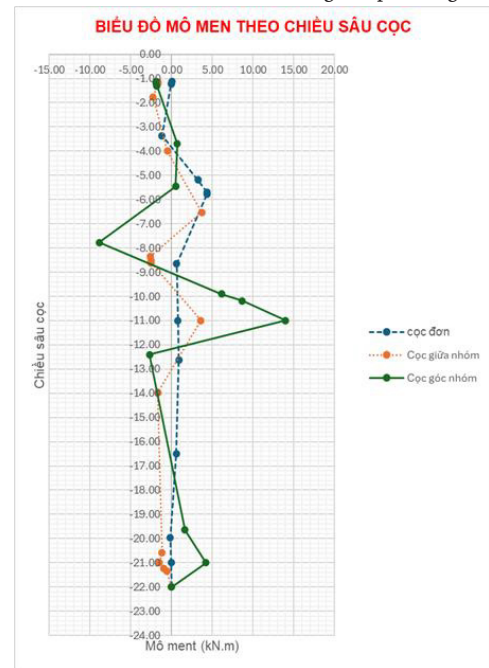
The diagrams indicate that the internal forces within the piles under dynamic seismic loading in the group case significantly increase compared to the single pile, with shear forces increasing by 192.5 % and bending moments by 72.4 %. However, the settlement of the pile group reduces by approximately 50 % compared to the single pile case.

During the time interval from 6 to 20 seconds, the ground surface displacement amplitude is observed to be 2.0 to 2.5 times greater than the average bedrock displacement amplitude. This indicates seismic wave amplification as the waves propagate through the soft soil layers, consistent with the wave propagation theory in soft soil.

According to the internal force distribution charts along the pile experience higher internal forces. This indicates that corner piles are more vulnerable during seismic events.



a. Shear force distribution along the pile length



b. Bending moment distribution along the pile

Figure 22. Internal force distribution along the pile depth.

4. Conclusions and Recommendations

This paper analyzed and evaluated the behavior of single rigid piles and pile groups in soft soil under seismic loading using a detailed 3D numerical model simulating the soil–pile–foundation interaction, while considering the nonlinear mechanical properties of soft soil subjected to earthquake excitation. The analysis results demonstrate a significant increase in internal forces within the pile shafts compared to static loading conditions, with shear forces and bending moments showing notable increments.

Due to the simultaneous time-dependent interaction between the pile system and the soil during seismic loading, internal forces also experience cyclic tension and compression over time. It is recommended that the design of pile foundation systems in soft soil environments be conducted using dynamic analysis methods to accurately assess the actual working behavior of the system. This ensures precision in computational modeling and foundation design, allowing the selection of appropriate values for pile foundation response under seismic loads, thus guaranteeing structural safety and design efficiency.

Acknowledgments

The author gratefully acknowledges Dong Thap University for supporting this research.

References

- [1]. Braja M. Das, *Principles of Foundation Engineering*, PWS.Engineering, 1984.
- [2]. Braja M. Das, *Principles of soil dynamics*, PWS-KENT Publishing Company, USA, 1995.
- [3]. Brinkgreve R.B.J. and Broere W., *Plaxis manual*, Delft University of technology & Plaxis b.v., The Netherlands, 2024.
- [4]. El-Sharnouby, B. and Novak, M., *Static and Low Frequency Response of Pile Groups*. Canadian Geotech. J., Vol. 22, No. 1, pp. 79-94, 1985.
- [5]. Fadeev A.B (1995), *Phương pháp phần tử hữu hạn trong địa cơ học (bản dịch)*, Nhà xuất bản Giáo Dục, Hà Nội.
- [6]. Gazetas, G. and Mylonakis, G., *Seismic Soil-Structure Interaction: New Evidence and Emerging Issues*. Geotechnical Earthquake Engineering and Soil Dynamics III: Proceedings of Specialty Conference, ASCE, 1998.
- [7]. <https://thanhvien.vn/nguy-co-dong-dat-o-viet-nam-co-dang-lo-185250330224850898.htm>
- [8]. Kramer, S. L., *Geotechnical Earthquake Engineering*. Prentice Hall, New Jersey, 1996.
- [9]. Lê Bảo Quốc, *Nghiên cứu phương pháp tính toán kết cấu công trình ngầm đô thị trong nền đất yếu chịu tác dụng của động đất*, Luận án tiến sỹ kỹ thuật, Học viện Kỹ thuật Quân sự, Hà Nội, 2016.
- [10]. Matlock, H. and Foo S. H. C., *Simulation of Lateral Pile Behavior under Earthquake Motion*. A Report to Chevron Oil Field Research Company La Habra, California. The University of Texas Austin, Department of Civil Engineering, 1978.
- [11]. Matlock, H., *Correlations for Design of Laterally Loaded Piles in Soft Clay*. Proc. Offshore Technology Conf., Houston, Texas, Vol. 1, Paper No. 1204, pp. 577-594, 1970.
- [12]. Nguyễn Lê Ninh, *Động đất và thiết kế công trình chịu động đất*, Nhà xuất bản xây dựng, 2007.
- [13]. TCVN-9386:2012. *Vietnam national standard - Design of structures for earthquake resistances*. Ministry of Science and Technology, 2012.
- [14]. Tiêu chuẩn quốc gia TCVN 10304: 2014, móng cọc tiêu chuẩn thiết kế.
- [15]. Verruijt A., *Soil dynamics*, Delft University of Technology, 1994, 2008.
- [16]. Zienkiewicz O.C. and Taylor R.L., *The Finite Element Method*, Vol 2: Solid Mechanics, Butterworth-Heinemann, A division of Reed Education and Professional Publishing Ltd, 2000.